Nano Select

RESEARCH ARTICLE OPEN ACCESS

Electronic Transport in AlGaN/GaN Nanowires Under Ultraviolet Excitation and Edge Depletion Effect, Studied in a Wide Temperature Range

Svetlana Vitusevich[1] | Vladislav V. Kaliuzhnyi[2] | Mykola D. Tymochko[2] | Alexander E. Belyaev[2]

[1]Institute of Biological Information Processing: Bioelectronics (IBI-3), Forschungszentrum Juelich, Juelich, Germany | [2]Department of kinetic phenomena and polaritonics, V. Lashkaryov Institute of Semiconductor Physics of National Academy of Sciences of Ukraine, Kyiv, Ukraine

Correspondence: Svetlana Vitusevich (s.vitusevich@fz-juelich.de)

Received: 23 September 2025 | **Revised:** 26 January 2026 | **Accepted:** 31 January 2026

Keywords: AlGaN/GaN nanowire | electronic transport | noise spectroscopy | space-charge-limited current (SCLC) | trap distribution | ultraviolet excitation

ABSTRACT

Gallium nitride (GaN) nanowires are promising for nanoelectronic and biosensing applications due to their unique electronic properties and stability. However, understanding electron transport in AlGaN/GaN nanowires, particularly the influence of edge depletion and trap states, remains limited. Here, we investigate electronic transport in AlGaN/GaN transistor-like heterostructures patterned into nanowires of varying widths (185–1110 nm), analyzing current–voltage characteristics under dark and ultraviolet (UV) illumination. External UV excitation influences the depletion widths in NWs, modulates space-charge-limited current (SCLC), and provides information about the distribution range of traps in NW structures. We observe a transition from Ohmic to SCLC regimes, with UV excitation modulating depletion widths and enhancing conductivity by releasing trapped carriers. Temperature-dependent measurements allow us to estimate trap energy distributions in the range of 150–200 meV, confirmed by noise spectroscopy data. These findings demonstrate that optical excitation effectively controls SCLC transport in GaN nanowires, offering insights for designing sensitive nanoelectronic and biosensing devices leveraging trap-mediated charge dynamics.

1 | Introduction

Gallium nitride (GaN) and its alloys have attracted significant attention in the semiconductor research community due to their unique material and electronic properties, which are valuable for a wide range of applications [1–3]. One-dimensional (1D) semiconductor nanowires (NWs) are promising candidates for electronic biosensors and are key elements in modern nanoelectronics, particularly for device miniaturization [4–6]. Their large surface-to-volume ratio enables efficient detection of targets at the atomic and molecular levels in biosensing applications. Recently, the space-charge-limited current (SCLC) effect, where current is limited by the presence of space charge due to injected carriers, has been observed in nanowire channels, including both GaN-based [7] and liquid-gated silicon nanowire channels [8–10]. The SCLC effect is highly sensitive to surface phenomena, making it a potential tool for detecting very small signals from biological objects [11, 12]. However, biosensors also require materials with high stability when in contact with biochemical liquids; GaN-based NWs are promising in this regard due to their wide band gap. Despite these advantages, the electron transport processes in NW biosensors are not yet fully understood, largely because their interfaces are extremely sensitive to surrounding materials and environmental conditions [4, 13]. Therefore, elucidations of temperature and light exposure effects on key electrical parameters, such as carrier density and mobility, in GaN-based NW structures represent important challenges. GaN-based NWs of different widths obtained by systematic top-down

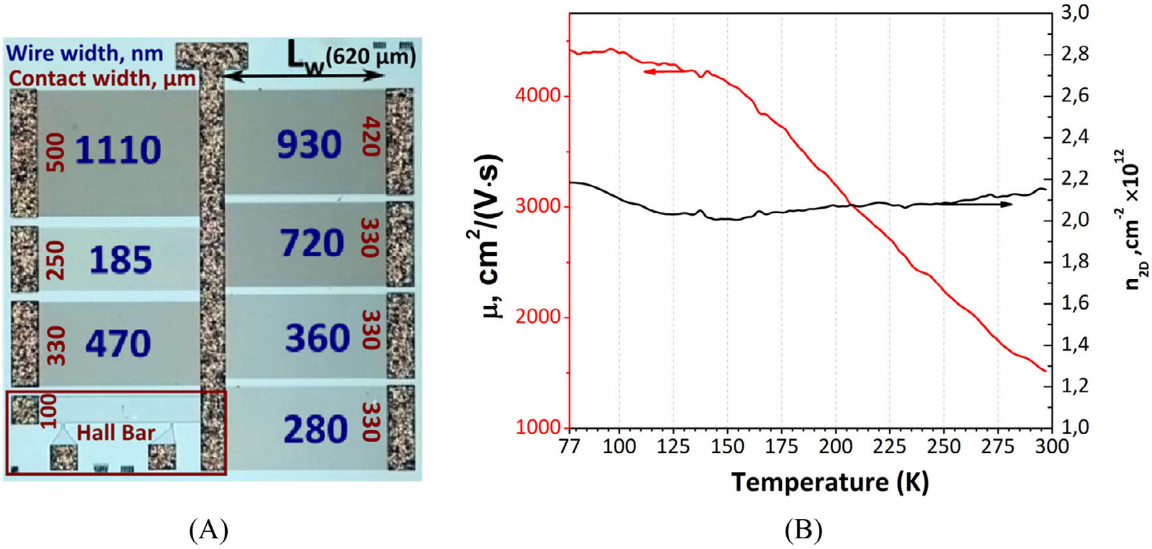

FIGURE 1 | (A) Schematic presentation of the nanowires of 620 μm length and different widths, W (nm): 1100, 930, 720, 470, 360, 280, and 185 listed in each set of nanowires with contact widths (μm): 500, 420, 330, 330, 330, 330, and 250 as well as a Hall bar structure, fabricated using AlGaN/GaN layer structure grown on a sapphire substrate. (B) Mobility, μ, and two-dimensional electron concentration, n_{2D}, as functions of temperature for the investigated AlGaN/GaN heterostructure.

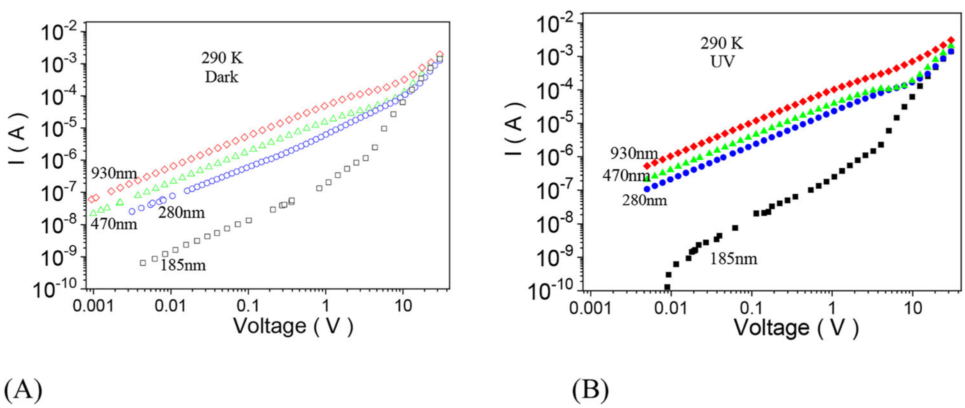

FIGURE 2 | Current–voltage characteristics of NW structures with various widths measured at 290K (A) in the dark and (B) under UV illumination using a 405 nm LED.

patterning of the same AlGaN/ GaN heterostructure represent perfect nanoscaled structures for studies of transport phenomena in comparison with GaN NWs of different diameters grown vertically.

In this work, we performed electrical characterization of AlGaN/GaN high-electron mobility transistor (HEMT) heterostructures patterned to NWs of various widths to investigate the features of electron transport in the structures at different temperatures and the influence of external light excitation, using light-emitting diodes (LED). Significant changes in the conductivity of the structures were revealed and explained by the modulation of the SCLC effect due to the effective change of charge carriers, which subsequently has an impact on electron transport in NW heterostructures. Temperature-dependent measurements of transport and noise properties using noise spectroscopy allowed us to estimate the trap energy distribution in the NW structures.

2 | Experimental Results and Discussion

Features of electron transport in AlGaN/GaN HEMT heterostructures patterned to NWs of various widths are investigated using current-voltage characteristics and noise spectra measured at different temperatures under the influence of light excitation and without it. The experimental samples with AlGaN/GaN NWs were fabricated using top-down technology. AlGaN/GaN HEMT heterostructures were grown by metal organic vapor phase epitaxy on a (0001) Al_2O_3 substrate. The layer structures included a 3-μm-thick GaN buffer, followed by a 40-nm-thick $Al_{0.1}Ga_{0.9}N$ barrier layer. The NWs were fabricated by patterning the prepared heterostructures using electron beam lithography and Ar^+ ion beam etching. The etching depth was ∼ 80 nm, meaning that the NWs include the heterojunction AlGaN/GaN with a 2DEG channel. Seven different sets of NWs were prepared. Each set consisted of $N = 160$ wires in parallel with a length (L) of 620 μm and varying widths (W: 185, 280, 360, 470, 720, 930, and

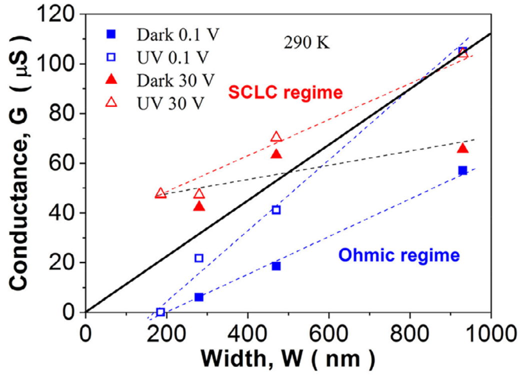

FIGURE 3 | Conductance as a function of NW width obtained in ohmic (squares) and SCLC (triangles) regimes in the dark (filled symbols) as well as under UV illumination (open symbols), measured at 0.1 and 30 V, respectively. The solid line represents the "nominal" conductance calculated using the charge carrier concentration and mobility obtained from Hall measurements.

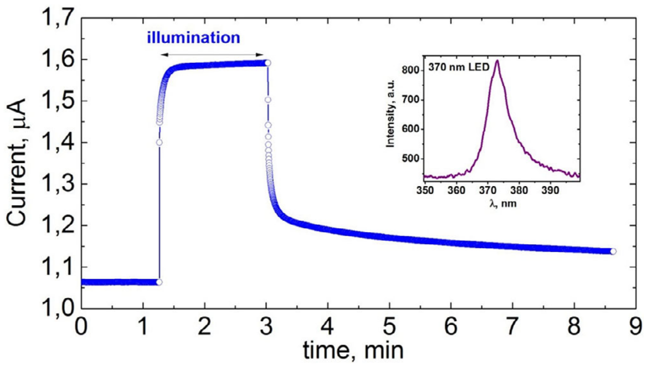

FIGURE 4 | Time dependence of the current before and after relatively brief UV photoexcitation using light with a wavelength of 370 nm. $T = 300$ K. Inset: characteristic spectrum of 370 nm UV LED illumination.

1110 nm). The long NW length (620 μm) was chosen to prevent the effect of contact resistance on the total NW resistance. Ohmic electrical contacts were formed by depositing Ti/Al/Ni/Au layers and subsequent annealing at 900°C for 30 s. Hall bar structures fabricated using the same AlGaN/GaN heterostructure were used to obtain the temperature dependencies of the two-dimensional (2D) carrier concentration, n_{2D}, and the mobility, μ (shown in Figure 1) via Hall measurements.

Electrical characterizations were performed using current–voltage (*I–V*) measurements of transmission line model (TLM) patterned structures. The contact resistivity was estimated to be 2×10^{-4} Ohm·cm^2, reflecting a negligibly small contribution from the contacts compared to the resistance of the NW conducting channel. The Stirling cooling system and vacuum chamber were used for lowering the temperature down to 70 K. Since the electrical characteristics of NWs have a strong dependence on external illumination and external conditions [14], the experimental setup with a closed vacuum chamber was used to prevent the impact of the external electromagnetic environment on the NW samples.

We used a blue-light ($\lambda = 460$–480 nm) and a set of UV LEDs with a narrow spectrum and peak wavelengths of 405, 370, and 365 nm. All LEDs have a similar optical power of ∼ 1 mW. The spectral range of the LEDs does not excite interband transitions and, at the same time, allows us to scan the distribution of traps over a wide range of energies in the band gap.

Initially, the time- and UV-wavelength dependencies of the current were studied. Significant changes in the conductivity of the structures were revealed under light excitation and upon decreasing the temperature. These findings are consistent with the modulation of the SCLC effect due to changes in charge carriers, which may impact electron transport in NW heterostructures.

Figure 2 shows the current–voltage characteristics of NWs with various widths measured in the dark and under UV illumination. At low bias (V<0.1 V), a linear regime corresponding to Ohmic behavior is registered. At higher bias, this linear dependence transforms into a superlinear behavior, indicating the formation of a (SCLC) regime with a power degree exceeding 2 and considerably low noise power spectral density [7, 15]. The onset of this effect clearly correlates with NW width. The smaller the width, the earlier the deviation from linear behavior begins. A strong change in the current, demonstrating the switching type, was observed for the narrower NW with a width of 185 nm.

The results obtained for conductivity, *G*, extracted from *I–V* characteristics at low voltages for planar GaN NWs of various widths, were used to estimate the depletion effects in the NWs. The extrapolation of *G(W)* to zero conductance (Figure 3, blue points) allowed us to estimate the width of a wire that cannot conduct electrical current, introduced as the "critical width," W_c. We consider our critical width, W_c, to correspond to the overall thickness of depletion regions on both sides of the nanowire ($W_c = 2W_{depl}$). The depletion width, Wdepl, in the dark is estimated to be 100 nm. We can therefore define the effective width of the conductive parts of the NWs as $W_{eff} = W - W_c$ and the aspect ratio as W_{eff}/W. Under UV illumination, W_c decreases to 180 nm (open rectangular blue symbols). This can be explained by the release of electrons from deep traps and surface levels. The results presented in Figure 3 confirm that in the linear regime, NW conductivity is determined by W_{eff}.

At high voltages (about $V = 30$ V) where the SCLC regime is fully formed [7, 15], the conductance exhibits a different dependence on NW width (Figure 3, red symbols), compared to both cases: under light excitation as well as in the dark at $V = 0.1$ V. It should be noted that at a voltage of 30 V, the electric fields in our long NWs are small enough, and hot-electron effects and related current nonlinearities are negligibly small [16]. Under dark conditions, the conductance demonstrates a slight decrease with decreasing NW width. Under UV light excitation, the conductance increases in the NW channels. It should be underlined that in nonlinear regions, the injected current flows through the entire cross-section of the sample.

The time dependence of the current relaxation after UV photoexcitation is investigated to evaluate the relaxation time of the samples (Figure 4).

Changes in currents upon illumination switch-on or switchoff can be well described by the stretched exponential relaxation

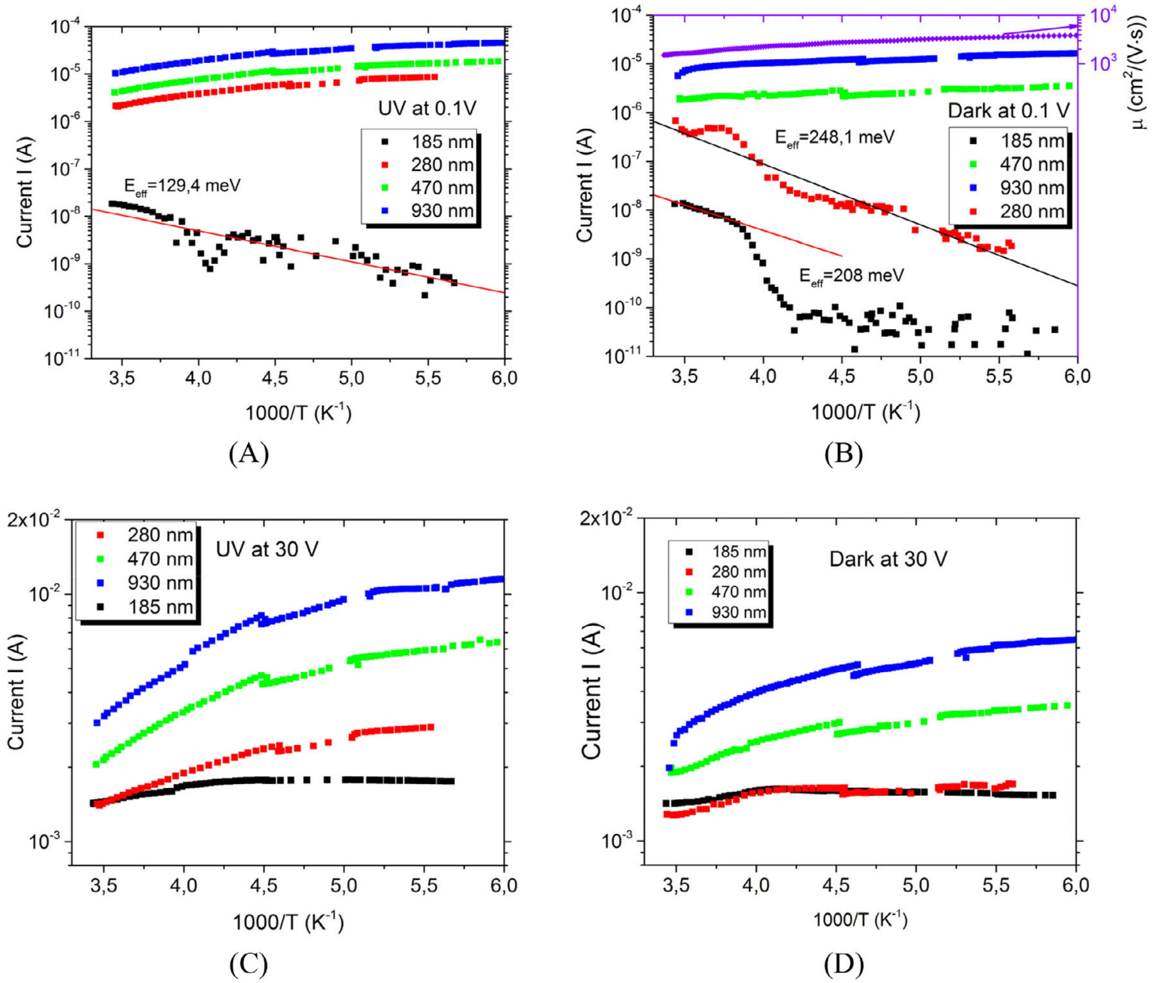

FIGURE 5 | Temperature dependences current of NWs with different widths measured in ohmic (A, B) and SCLC (C, D) regimes in the dark (B, D) and under UV illumination (A, C). Solid lines represent Arrhenius fitting. Graph 5B shows the dependence of mobility on the inverse temperature for comparison (magenta points, right axis).

function [17]

$$f_{\beta}(t) = e^{-t^{\beta}}$$

where β is the fractional fixed power inserted in the exponential function "f" as a function of time, t.

The observed relaxation process, which follows a stretched exponential form, is consistent with models commonly used to describe relaxation in disordered systems. In such systems, the overall relaxation arises from the combined effect of many independently relaxing species, each decaying exponentially with its own characteristic rate [18–20]. This approach effectively captures the broad energy distribution of traps present in GaN-based NWs.

The conductance of the multi-NW structure can be defined as $G_0 = \mathrm{eN}\mu \mathrm{n_{2D}W/L}$. Using experimental values of mobility (μ) and the concentration of 2DEG (n_{2D}), we can plot the nominal current flow $G(W)$ dependence (depicted in Figure 3 by a solid line). Assuming that the carrier concentration and mobility do not change, the conductance of the NWs can approach the calculated values in the case of the SCLC regime, whereas it approaches values reduced by W_{eff}/W, relative to nominal conductivities, in the case of the ohmic regime. Although the conductivities measured in both regimes—ohmic and nonlinear (in the dark)—follow the aspect ratio behavior, their values $G(W)$ differ significantly from those that were calculated. At the same time, under illumination, the experimental conductivities approach nominal values, indicating that nearly the full width of the NWs becomes conductive for charge-carrier transport.

The results presented above show that traps play a significant role in determining the current–voltage characteristics. In particular, this is the case for patterned NWs, irrespective of the trap distribution, whether it be exponential, Gaussian, uniform, or discrete in energy. The characteristics of the trap energy range in these nanomaterials can be extracted by analyzing the temperature-dependent I–V characteristics [21–25]. The temperature-dependent responses for NWs of different widths are shown in Figure 5.

The temperature dependence of the current (conductivity) differs notably between NWs of varying widths. For NWs with widths of 280 nm and above, the effective conduction channel is sufficiently wide, and the temperature dependence of conductivity resembles that of a two-dimensional electron gas (2DEG), where

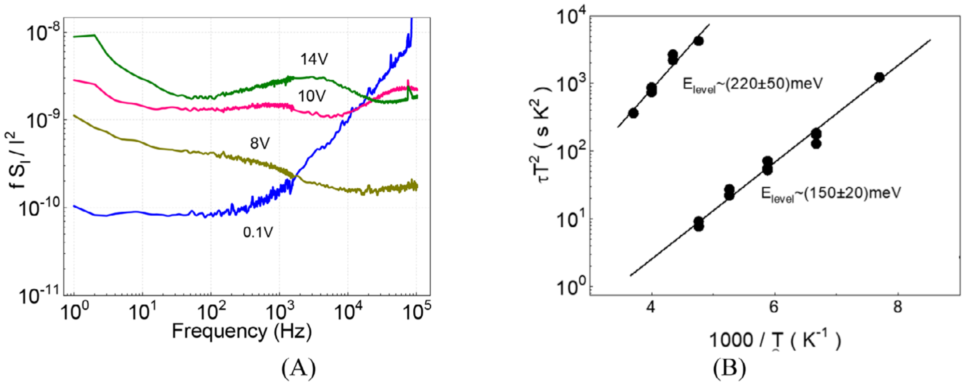

FIGURE 6 | (A) Normalized noise spectra, measured for AlGaN/GaN sample with 620 um length and 1100 nm width at different applied voltages at room temperature, demonstrating very well-resolved Lorentzian noise components registered at relatively large voltages, corresponding to formation of SCLC regime, (B) Arrhenius plots obtained using Lorentzian noise components of noise spectra, measured in a wide temperature range allows us to estimate energies of traps responsible for registered bumps in the noise spectra.

conductivity decreases as the temperature increases. In contrast, for the 185 nm wide NW, conductivity increases with increasing temperature. This behavior can be explained by considering that, in the GaN/AlGaN heterostructure, increasing temperature leads not only to a higher concentration of charge carriers at the interface but also to increased scattering, thereby reducing mobility. Since channel conductivity is proportional to the product $\sigma \sim e\mu n_s$ (where μ is the mobility and n_s is the surface concentration of charge carriers), a decrease in conductivity with temperature indicates that the reduction in mobility outweighs the increase in carrier concentration. The traps are involved in the formation of depletion regions at the NW edges, which may confine two-dimensional gas conductivity to restricted regions.

Under light excitation, increased current flow is observed in patterned NW regions, resulting in modulation of the SCLC regime in GaN-based NW structures. For this reason, we were able to estimate the effective trap energy for these thinnest NWs, in which temperature changes in concentration dominate changes in mobility. Using Arrhenius plots for NWs with a width of 185 nm, the characteristic energy of edge traps, $E_{eff,}$ in GaN-based NWs was determined to be in the range of 130–250 meV. As all NW channels of different widths were fabricated simultaneously using Ar+ ion beam etching, these energy levels are expected to influence the transport regimes across all NWs. Traps are crucial in forming depletion regions at the NW edges, effectively confining the two-dimensional electron gas and restricting conductivity to quasi-one-dimensional (1D) transport regimes. Modeling of electronic band banding supports the contribution of traps on sidewall states into the formation of low-dimensionality channels in NWs of different widths [15]. Upon light excitation, the entire cross-section of the patterned NWs becomes conductive, leading to strong modulation of the SCLC regime in GaN-based NW structures.

Moreover, these results are confirmed by studies of AlGaN/GaN NWs using noise spectroscopy data. Figure 6A shows typical selected noise spectra reflecting features of registered noise spectra corresponding to low voltage linear regime, as well as to relatively high voltages, corresponding to observed SCLC regime at room temperature. The spectra were measured using our home-made measurement setup [26] in the frequency range from 1 Hz to 100 kHz at different temperatures. Very well-resolved Lorentzian noise components are registered with increased voltages on top of the flicker noise component. Analysis of frequency position corresponding to the maximum of the Lorentzian noise component as a function of frequency allows us to estimate the characteristic energy of traps using Arrhenius plots (Figure 6B).

Two energy levels are obtained: 150 meV and 220 meV, which are in good agreement with trap energies obtained for the sample with the smallest width described above. The results confirm the feasibility and reliability of the formation of the SCLC regime stipulated by the controlled influence of external optical excitation on traps. Strong modulation effect enables the effective tuning of the SCLC transport regime, which is important for numerous practical applications.

3 | Conclusion

In conclusion, we investigated electron transport phenomena in AlGaN/GaN NWs of varying widths over a wide temperature range, both in the dark and under UV optical excitation. Our analysis, focused on static edge-trap-induced charge redistribution, enabled estimation of depletion effects at low voltages and revealed a transition from linear to SCLC regimes at high voltages. Temperature-dependent measurements allowed us to estimate the trap energy distribution in the NWs to be 130–250 meV. This finding is confirmed by a careful analysis of the noise-spectroscopy data obtained at different temperatures. UV light excitation produced a strong modulation effect, enabling effective tuning of the SCLC transport regime. These findings are promising for the development of novel nanoelectronic, photonic, and biosensing device structures.

Acknowledgments

This study was supported by the National Academy of Sciences of Ukraine (Project No. 4.11/23-P). A.E.B. gratefully acknowledges the long-term program supporting the Ukrainian research teams at the Polish Academy of Sciences, which was carried out in collaboration with the U.S. National Academy of Sciences with the financial support of external partners (Project: LTP NAS KOCHELAP A7.11.0008; contract # PAN.BFB.S.BWZ.367.022.2023). The authors would also like to thank T. Schäpers for the valuable collaborative work.

Open access funding enabled and organized by Projekt DEAL.

Conflicts of Interest

The authors declare no conflicts of interest.

Data Availability Statement

The data that support the findings of this study are available from the corresponding author upon reasonable request.

References

1. N. Islam, M. F. P. Mohamed, M. Khan, S. Falina, H. Kawarada, and M. Syamsul, "Reliability, Applications and Challenges of GaN HEMT Technology for Modern Power Devices: A Review," *Crystals* 12 (2022): 1581, https://doi.org/10.3390/cryst12111581.

2. S. Vitusevich, I. M. Nasieka, A. V. Naumov, et al., "Thermometry of AlGaN/GaN Two-Dimensional Channels at High Electric Fields Using Electrical and Optical Methods," *Advanced Electronic Materials* 9, no. 6 (2023): 2201330, https://doi.org/10.1002/aelm.202201330.

3. M. Riedel, S. Hölzel, P. Hille, J. Schörmann, M. Eickhoff, and F. Lisdat, "InGaN/GaN Nanowires as a New Platform for Photoelectrochemical Sensors—Detection of NADH," *Biosensors and Bioelectronics* 94 (2017): 298–304, https://doi.org/10.1016/j.bios.2017.03.022.

4. N. P. Dasgupta, J. Sun, C. Liu, et al., "25th Anniversary Article: Semiconductor Nanowires—Synthesis, Characterization, and Applications," *Advanced Materials* 26 (2014): 2137–2184, https://doi.org/10.1002/adma.201305929.

5. E. Barrigon, M. Heurlin, Z. Bi, B. Monemar, and L. Samuelson, "Synthesis and Application of III-V Nanowires," *Chemical Reviews* 119 (2019): 9170–9220, https://doi.org/10.1021/acs.chemrev.9b00075.

6. C. P. Chen, A. Ganguly, C. Y. Lu, et al., "Ultrasensitive In Situ Label-Free DNA Detection Using a GaN Nanowire-Based Extended-Gate Field-Effect-Transistor Sensor," *Analytical Chemistry* 83 (2011): 1938–1943, https://doi.org/10.1021/ac102489y.

7. V. A. Sydoruk, S. A. Vitusevich, H. Hardtdegen, et al., "Electric Current and Noise in Long GaN Nanowires in the Space-Charge Limited Transport Regime," *Fluctuation and Noise Letters* 16 (2017): 1750010, https://doi.org/10.1142/S0219477517500109.

8. Y. Zhang, K. Li, N. Boichuk, et al., "Impact of Light Excitation on Liquid Gate-All-Around Silicon Nanowire Field-Effect Transistor Biosensors With Bowtie," *Antenna Advanced Material Technologies* 10 (2025): 2400747, https://doi.org/10.1002/admt.202400747.

9. Y. Zhang, N. Boichuk, D. Pustovyi, et al., "Peculiarities of the SCLC Effect in Gate-All-Around Silicon Nanowire Field-Effect Transistor Biosensors," *Advanced Electronic Materials* 10, no. 7 (2014): 2300855, https://doi.org/10.1002/aelm.202300855.

10. M. Petrychuk, D. Pustovyi, N. Boichuk, Y. Zhang, H. Long, and S. Vitusevich, "New Approach for Enhancing Sensitivity in Liquid-Gated Nanowire FET Biosensors under Optical Excitation," *Advanced Materials Technologies* 9 (2024): 2301303, https://doi.org/10.1002/admt.202301303.

11. A. Ahmadivand, R. Sinha, S. Kaya, and N. Pala, "Rhodium Plasmonics for Deep-Ultraviolet Bio-Chemical Sensing," *Plasmonics* 11 (2016): 839–849, https://doi.org/10.1007/s11468-015-0117-x.

12. M. R. Hajinezhad, M. Barani, and S. Sargazi, "Histopathological and Biochemical Profiling of Carfilzomib-Loaded Fe-Co MOFs," *Discover Nano* 20 (2025): 135, https://doi.org/10.1186/s11671-025-04334-3.

13. P. Yang, R. Yan, and M. Fardy, "Semiconductor Nanowire: What's next?," *Nano Letters* 10 (2010): 1529–1536, https://doi.org/10.1021/nl100665r.

14. C. Pfüller, O. Brandt, F. Grosse, et al., "Unpinning the Fermi Level of GaN Nanowires by Ultraviolet Radiation," *Physical Review B* 82 (2010): 045320, https://doi.org/10.1103/PhysRevB.82.045320.

15. V. A. Sydoruk, I. Zadorozhnyi, H. Hardtdegen, et al., "Electronic Edge-State and Space-charge Phenomena in Long GaN Nanowires and Nanoribbons," *Nanotechnology* 28 (2017): 135204, https://doi.org/10.1088/1361-6528/aa5de3.

16. S. A. Vitusevich, S. V. Danylyuk, N. Klein, et al., "Separation of Hot-Electron and Self-Heating Effects in Two-Dimensional AlGaN/GaN-Based Conducting Channels," *Applied Physics Letters* 82 (2003): 748–750, https://doi.org/10.1063/1.1542928.

17. D. C. Johnston, "Stretched Exponential Relaxation Arising From a Continuous Sum of Exponential Decays," *Physical Review B* 74 (2006): 184430, https://doi.org/10.1103/PhysRevB.74.184430.

18. R. J. Freitas and K. Shimakawa, "Kinetics of the Persistent Photoconductivity in Crystalline III-V Semiconductors," in *Optical Properties of Materials and Their Applications*, J. Singh (John Wiley & Sons, Ltd, 2019): 611–626, https://doi.org/10.1002/9781119506003.CH20. ch. 20.

19. S. Cai, B. D. Nener, J. M. Dell, and L. Faraone, "Kinetics of Persistent Photoconductivity in GaN Grown by MOCVD," in *COMMAD 2000 Proceedings. Conference on Optoelectronic and Microelectronic Materials and Devices, Bundoora, VIC, Australia* (IEEE, 2000), 165–168, https://doi.org/10.1109/COMMAD.2000.1022917.

20. S. Ghosh and V. Kumar, "Stretched Exponential Relaxation of Persistent Photoconductivity due to the Si-Related DX Centre in AlxGa1?XAs," *Europhysics Letters* 24 (1993): 779–784, https://doi.org/10.1209/0295-5075/24/9/014.

21. A. D. Schricker, F. M. Davidson III, R. J. Wiacek, and B. A. Korgel, "Space Charge Limited Currents and Trap Concentrations in GaAs Nanowires," *Nanotechnology* 17 (2006): 2681–2688, https://doi.org/10.1088/0957-4484/17/10/040.

22. V. Kumar, S. C. Jain, A. K. Kapoor, J. Poortmans, and R. Mertens, "Trap Density in Conducting Organic Semiconductors Determined From Temperature Dependence of J-V Characteristics," *Journal of Applied Physics* 94 (2003): 1283–1285, https://doi.org/10.1063/1.1582552.

23. B. S. Simpkins, M. A. Mastro, C. R. Eddy Jr., J. K. Hite, and P. E. Pehrsson, "Space-Charge-Limited Currents and Trap Characterization in Coaxial AlGaN/GaN Nanowires," *Journal of Applied Physics* 110 (2011): 044303, https://doi.org/10.1063/1.3622145.

24. O. Mitrofanov and M. Manfra, "Poole-Frenkel Electron Emission From the Traps in AlGaN/GaN Transistors," *Journal of Applied Physics* 95 (2004): 6414–6419, https://doi.org/10.1063/1.1719264.

25. S. Yang, C. Zhou, Q. Jiang, J. Lu, B. Huang, and K. J. Chen, "Investigation of Buffer Traps in AlGaN/GaN-On-Si Devices by Thermally Stimulated Current Spectroscopy and Back-Gating Measurement," *Applied Physics Letters* 104 (2014): 013504, https://doi.org/10.1063/1.4861116.

26. S. Pud, J. Li, M. Petrychuk, et al., "Modulation Phenomena in Si Nanowire FETs Characterized Using Noise Spectroscopy and Gamma Radiation Technique," *Journal of Applied Physics* 113 (2013): 124503, https://doi.org/10.1063/1.4795603.